scientific reports

Check for updates

OPEN

Single-nucleus RNA sequencing uncovers metabolic dysregulation in the prefrontal cortex of major depressive disorder patients

Xiang-Yao Li[1,2]✉, Yingbo Rao[3], Guo-Hao Li[1], Luxi He[1], Yaohan Wang[1], Wenli He[1], Ping Fang[1], Chenyu Pei[1,2], Lun Xi[1], Haiyan Xie[1] & Yun-Rong Lu[1,4]✉

Major depressive disorder (MDD) is a widespread psychiatric condition, recognized as the third leading cause of global disease burden in 2008. In the context of MDD, alterations in synaptic transmission within the prefrontal cortex (PFC) are associated with PFC hypoactivation, a key factor in cognitive function and mood regulation. Given the high energy demands of the central nervous system, these synaptic changes suggest a metabolic imbalance within the PFC of MDD patients. However, the cellular mechanisms underlying this metabolic dysregulation remain not fully elucidated. This study employs single-nucleus RNA sequencing (snRNA-seq) data to predict metabolic alterations in the dorsolateral PFC (DLPFC) of MDD patients. Our analysis revealed cell type-specific metabolic patterns, notably the disruption of oxidative phosphorylation and carbohydrate metabolism in the DLPFC of MDD patients. Gene set enrichment analysis based on human phenotype ontology predicted alterations in serum lactate levels in MDD patients, corroborated by the observed decrease in lactate levels in MDD patients compared to 47 age-matched healthy controls (HCs). This transcriptional analysis offers novel insights into the metabolic disturbances associated with MDD and the energy dynamics underlying DLPFC hypoactivation. These findings are instrumental for comprehending the pathophysiology of MDD and may guide the development of innovative therapeutic strategies.

Keywords SnRNA-Seq, Major depressive disorder, Serum lactate, Glycolysis, KEGG

Major depressive disorder (MDD) is a highly prevalent psychiatric disorder that was the third most common cause of disease burden worldwide in 2008, according to the World Health Organization (WHO), and this disease will rank first by 2030[1]. The lifetime incidence of MDD is approximately 12%. Approximately 30% of people with MDD are resistant to conventional treatments[2,3]. The prefrontal cortex (PFC) is critical for multiple brain functions, such as regulating cognition, emotion, and behavior[4]. Both preclinical and clinical studies have shown hypoactivation of the PFC in MDD[4,5]. Patients with MDD exhibit significantly decreased gray matter volume and glutamate-related synaptic transmission in the PFC[6]. Preclinical studies using a rodent depression model showed decreased dendritic spine numbers in the PFC[7]. A low level of spinogenesis was correlated with depression-related behavior, while antidepressant-dose ketamine rescued spine elimination and restored coordinated activity[8]. Thus, a lower level of glutamate excitatory neurotransmission in the PFC leads to PFC hypoactivity, which contributes to the development and maintenance of MDD[5,9].

Synaptic transmissions in the brain consume most of the energy supplied in the central nervous system (CNS)[10]. The energy supply affects presynaptic neuronal transmitter release[11] and determines postsynaptic plasticity[12]. Conversely, a lower level of excitatory synaptic transmission in MDD indicates a decrease in energy consumption in the PFC. Recent studies have shown abnormal metabolism[13–15], including the kynurenine pathway[16–18] and glucose metabolism[19–21], in MDD patients. The abnormal glucose metabolism in the brains

[1]Department of Psychiatry, The Fourth Affiliated Hospital of School of Medicine, and International School of Medicine, International Institutes of Medicine, Zhejiang University, Yiwu 322000, China. [2]NHC and CAMS Key Laboratory of Medical Neurobiology, MOE Frontier Science Center for Brain, Research and Brain-Machine Integration, School of Brain Science and Brain Medicine, Zhejiang University, Hangzhou 310058, Zhejiang, China. [3]Department of Clinical Laboratory, The Fourth Affiliated Hospital of School of Medicine, and International School of Medicine, International Institutes of Medicine, Zhejiang University, Yiwu 322000, China. [4]Department of Psychiatry, The Second Affiliated Hospital, Zhejiang University School of Medicine, Hangzhou 310009, Zhejiang, China. ✉email: Lixiangy@zju.edu.cn; 2201005@zju.edu.cn

of diabetes patients may lead to anomalous cognition[22]. Additionally, stress impairs synaptic plasticity via the astrocytic energy reservoir[23]; fasting improves cognitive-affective sub-scores in MDD patients with moderate/severe symptoms[24]. These findings suggest that both impaired synaptic transmission and impaired metabolism may contribute to the development and maintenance of MDD. However, the cellular mechanisms mediating the metabolic changes in the CNS of MDD patients have not been elucidated.

Lactate, historically considered a mere byproduct of glycolysis, now stands as a pivotal metabolite in the brain, serving dual roles as both an energy substrate and a signaling molecule. Central to the astrocyte-neuron lactate shuttle (ANLS), lactate is instrumental in shuttling energy from astrocytes to neurons, underpinning synaptic transmission and neuronal metabolism, especially during heightened metabolic activity[25]. The ANLS ensures that neurons receive a consistent supply of lactate to satisfy their bioenergetic necessities, highlighting the importance of lactate in brain function and disease[26]. The research underscores lactate's significance in brain development, synaptic plasticity, angiogenesis, and the pathogenesis of neurodegenerative diseases, with disruptions in lactate metabolism linked to cognitive decline and neurodegenerative conditions[27]. These positions lactate not only as a critical component of brain metabolism but also as a potential therapeutic target for bolstering brain energy and defending against neurodegenerative insults[25–28].

Single-cell RNA sequencing (scRNA-seq) or single-nucleus RNA sequencing (snRNA-seq) approaches have unraveled psychiatric disorders' molecular and cellular mechanisms, including MDD[29]. Applying the RNA-seq approach at the cellular level helps to understand the cellular heterogeneity of neuroanatomical regions and provides cell type-dependent transcriptomic change information for MDD patients. A recent study offered transcriptional profiling of the mouse habenula complex[30], while the associations of somatostatin interneurons and astrocytes with depression were also explored[31]. The results of snRNA-seq in the DLPFC indicate the dysregulation of deep-layer excitatory neurons and immature oligodendrocyte precursor cells (OPCs) in MDD patients[32] and the difference between males and females[33]. Furthermore, transcriptional profiling also provides clues about metabolic information[34]. Here, we performed a metabolic-related analysis based on the published snRNA-seq database of the DLPFC from MDDs and HCs. Our results indicated impaired oxidative phosphorylation and carbohydrate metabolism in the DLPFC. Our study thus provides transcriptional information about the abnormal metabolism in the DLPFC of MDD patients.

Methods

Resources of snRNA-seq data

The snRNA-seq datasets (raw or gene expression matrices) of the human dorsolateral prefrontal cortex (DLPFC) used in this study were downloaded from the NCBI Gene Expression Omnibus (GEO) database under accession numbers GSE144136[32], comprising a total of 17 MDD patients and 14 healthy controls (HCs) samples. Prior to data integration, we excluded low-quality cells using the Seurat package (v.4.3.0.1). Only cells expressing more than 200 genes but fewer than 6,000 genes were included, and only genes expressed in at least three single cells (0.1% of the raw data) were retained for further analysis. The preprocessing of the snRNA-seq followed a similar approach to our previous study[35]. We excluded cells expressing hemoglobin genes (*HBM*, *HBA1*, *HBA2*, *HBB*, *HBD*, *HBE1*, *HBG1*, *HBG2*, *HBQ1*, and *HBZ*) , indicative of red blood cells. Cells with a mitochondrial gene percentage exceeding 10% were also discarded. We used the DecontX function from the Celda R package (v.1.12.0), a Bayesian method, to estimate and remove RNA contamination in individual cells without empty droplet information. Additionally, we employed the DoubletFinder R package (v.2.0.3) with a doublet rate of 7.5% to detect and eliminate doublets[36]. The Harmony R package (v.0.1.1) was used to adjust for batch effects. After these steps, 36,588 genes across 69,257 nuclei (HC:29,979 nuclei, MDD: 39,278 nuclei) remained for subsequent analysis. The data were normalized to a sequencing depth of 1×10^4 molecules per cell using the Seurat package (v.4.3.0.1).

Identification of cell types and subtypes

We employed the Seurat package (v.4.3.0.1) for linear dimensional reduction, selecting 2000 highly variable genes as input for principal component analysis (PCA). Significant principal components (PCs) were identified using the JackStrawPlot function. Subsequently, Harmony integration was performed based on PCA, followed by t-SNE and UMAP dimensional reduction on strong PCs (PC1–PC50). Cells were clustered using the FindClusters function with a resolution of 0.4. Clusters were annotated based on known cell-type markers[33], including *PDGFRA* (oligodendrocyte precursor cells, OPC), *CLDN5* (endothelial cells, Edn), *LRMDA* (microglia, MIC), *GJA1* (astrocytes, ASC), *CLDN11* (oligodendrocytes, OLG), *SLC17A6/SLC17A7* (glutamatergic neurons, ExNs), and *GAD1/GAD2* (GABAergic neurons, InNs).

Identification of DEGs

Differentially expressed genes (DEGs) for each cluster were identified using the FindMarkers function (thresh.use = 0.25, test.use = "Wilcox") in the Seurat package (v.4.3.0.1). Genes with an average expression difference > 0.25 natural log and $P < 0.05$ were selected as marker genes. To compare MDD and HC samples, we performed the Wilcoxon rank-sum test using the FindMarkers function. Additionally, we analyzed differential gene expression via a pseudobulk approach. The Muscat package (v.1.18.0) in Bioconductor was utilized to identify DEGs across conditions within specific cell types or clusters from single-cell RNA-sequencing (scRNA-seq) data. The scRNA-seq data were preprocessed into a SingleCellExperiment object, and pseudobulk data were generated for each cluster and sample using the aggregateData function. Differential State (DS) analysis was performed on the pseudobulk data using the pbDS function, and significant DEGs were filtered based on adjusted p-values and log fold changes. The results were formatted using the resDS function for further analysis. The statistical thresholds for identifying significant DEGs were set to $|avg\_log2FC| > 0.25$ and $p\_val\_adj < 0.05$.

Metabolism and human phenotype ontology (HPO) analysis

Metabolism-related terms and genes were retrieved using the KEGGREST R package (v.1.36.0) and EnrichmentBrowser R package (v.2.22.2) from the Kyoto Encyclopedia of Genes and Genomes (KEGG) database. Specifically, terms containing "hsa00" were selected for further analysis. Cell-type-dependent metabolic analysis was conducted using the AddModuleScore function from the Seurat package (v.4.3.0.1), with reaction and pathway data obtained via the ReactomePA (v.1.42.0)[37] and Reactome.db (v.1.82.0) R packages. Differences between MDD and HCs were assessed using the FindMarkers function (thresh.use = 0.25, test.use = "Wilcox") in the Seurat R package (v.4.3.0.1). Gene Set Enrichment Analysis (GSEA) was performed using the fgsea R package (v.1.25.1). The Human Phenotype Ontology datasets[38] were downloaded from the MSigDB database. GSEA on HPO terms was conducted using the gsea function from the clusterProfiler R package (v.4.12.0).

The metaFlux R package

Flux balance analysis and metabolic network reconstructions

Flux balance analysis (FBA) and genome-scale metabolic network reconstructions[39] were performed using the METAflux R package (v.0.0.0.9000). The Human-GEM[40] was utilized as the underlying metabolic model. The average expression levels of genes within each cell type were calculated using the calculate_avg_exp function on our Seurat object, with 60 bootstrap iterations and a random seed of 1 to ensure reproducibility. Reaction scores were subsequently computed from these mean expression values using the calculate_reaction_score function. The proportion of each cell type was estimated by tabulating the cell type distribution and normalizing it by the total number of cells. These proportions were used to compute the single-cell flux with the compute_sc_flux function, considering a specified number of cells and their respective flux scores in the context of the human blood medium.

Visualization and statistical analysis of metabolic flux

To visualize and statistically assess the differences in metabolic flux between HCs and MDD patients, the flux data were first transformed using a cube root transformation to stabilize the variance. Glucose-related flux data were extracted and reshaped into a long format, with conditions (HC or MDD) assigned to each data point. These datasets were combined, and numeric cell-type identifiers were replaced with descriptive labels. Boxplots and violin plots of the flux values for each cell type, colored by condition, were generated using ggplot2 (v.3.5.1). Wilcoxon tests were performed to compare the flux values between conditions, with significance levels annotated on the plots.

Jaccard analysis

The Jaccard similarity coefficient was employed to assess the similarity between the featured DEGs of our datasets and those from previous research. The Jaccard coefficient measures the similarity between finite sample sets and is defined as the size of the intersection divided by the size of the union of the sample sets. Unique clusters in each dataset were identified by tabulating the cluster assignments of genes in df_gene1 and df_gene2. An empty vector df_ja was initialized to store the Jaccard coefficients for each pair of clusters. For each cluster *i* in df_gene1, the gene list was extracted and compared with each cluster *j* in df_gene2. The Jaccard coefficient was calculated as the ratio of the number of common genes (intersection) to the total number of unique genes (union) across both clusters. These coefficients were stored in a matrix and visualized using the pheatmap package in R.

Experiments for the serum lactate examination on human

Participant population

The present study recruited patients diagnosed with MDD from the Department of Psychiatry of the Fourth Affiliated Hospital, Zhejiang University School of Medicine (Yiwu, China), between January to July 2024. The study was conducted in accordance with the latest version of the Declaration of Helsinki, and all participants provided informed consent. The study was approved by the ethical committee of the Fourth Affiliated Hospital, Zhejiang University School of Medicine (K2024157). MDD was diagnosed by qualified psychiatrists according to the International Statistical Classification of Diseases and Related Health Problems, 10th Revision (ICD-10). The Chinese version of the 24-Hamilton depression scale (HAMD-24) was used to assess clinical symptoms.
Inclusion criteria:

1. Adult patients aged 13–60 years.
2. HAMD score ≥ 20.
3. Patients not receiving any antipsychotic medications or other medications that could influence lactate levels.

Exclusion criteria:

1. Participants with any organic psychiatric disorder, schizophrenia, bipolar disorder, or mental retardation.
2. Participants with psychiatric comorbidities, such as substance abuse disorders.
3. Participants with chronic physical illness.
4. Pregnant or breastfeeding women.
5. HCs with a family history of mental illness.

Sample collection and measurements

Fasting peripheral venous blood samples (5 mL) were collected via venipuncture between 07:00 and 09:00 AM. Serum was obtained by centrifugation at 3000 rpm for 15 min, separated into aliquots, and stored at − 80 °C until laboratory assays. Serum lactate levels were measured using an L-lactic acid (LA) Colorimetric Assay Kit

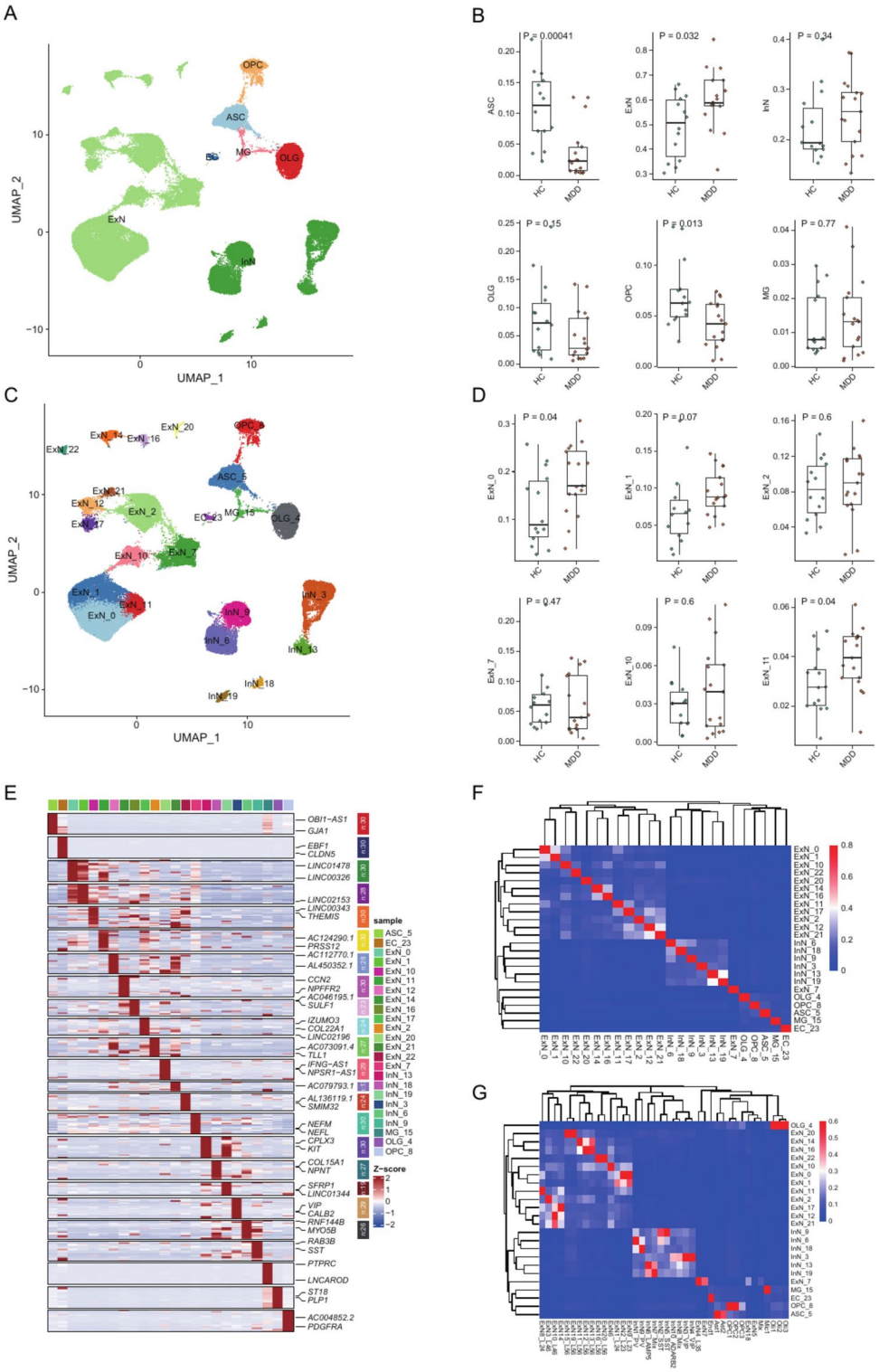

(E-BC-K044-S, Elabscience) according to the manufacturer's instructions. Assays were performed by the same technician, who was blinded to the sample's ID and clinical information.

Statistical analysis

All analyses were conducted using the R environment (R, 4.4.1). Demographic and clinical characteristics of MDD patients and HCs were described. Categorical variables were analyzed using the chi-square test. Pearson correlation analysis was used to assess the correlations between serum lactate levels in MDDs and HCs. A p-value < 0.05 was considered statistically significant.

◀**Fig. 1**. Single-Cell Transcriptomic Profiles of dorsolateral Prefrontal Cortex (DLPFC) Cells (**A**) Umap embedding projection depicting seven distinct cell types from single-cell RNA-sequencing (scRNA-seq) data of PFC samples from HCs and MDD patients. (ExN: glutamatergic neurons; InN: GABAergic neurons; OLG: oligodendrocytes; ASC: astrocytes; OPC: oligodendrocyte precursor cells; MG: microglia; EC: endothelial cells). (**B**) Boxplots representing the percentage differences in cell type distribution between HCs and MDD groups. The central line of box plots represents the median, and the boxes represent the Interquartile range (IQR). (**C**) Umap embedding projection illustrating the subtypes of cells derived from single-cell RNA-sequencing (scRNA-seq) data of DLPFC samples from HCs and MDDs. (**D**) Boxplots showing the percentage differences in cell subtype distribution between HC and MDD groups. The central line of box plots represents the median, and the boxes represent the IQR. (**E**) Heatmap displaying the relative expression levels of focal differentially expressed genes (fDEGs) across cell subtypes. (**F**) Heatmap representing the correlation of fDEGs among various cell subtypes. (**G**) Heatmap indicating the correlation of fDEGs from cell subtypes to those identified in previously published studies.

Results

The integrated dataset revealed the major cell types in the DLPFC

After removing RNA contamination in individual cells and deleting the doublet cells, we integrated the snRNA-seq datasets of the human DLPFC[32] based on samples and conditions (HCs and MDD, Supplementary Table 1) via the Harmony R package (v.0.1.1). We further detected cell clusters via the FindClusters function of the Seurat R package and identified 24 clusters at a resolution of 0.4. In total, 36,588 genes across 69,257 nuclei (HC: 29,979 nuclei, MDD: 39,278 nuclei) remained for subsequent analysis. Based on previous studies[32], we annotated the major cell types in the DLPFC (Fig. 1A), including oligodendrocyte precursor cells (OPC, *PDGFRA*$^+$), endothelial cells (EC, *CLDN5*$^+$), microglia (MG, *LRMDA*$^+$), astrocytes (ASC, *GJA1*$^+$), oligodendrocytes (OLG, *CLDN11*$^+$), excitatory neurons (ExN, *SLC17A6*$^+$, *SLC17A7*$^+$), and inhibitory neurons (InN, *GAD1*$^+$, *GAD2*$^+$). We also estimated cell-type proportions and observed differences in ASC, ExN, and OPC proportions between the MDD and HC groups (Fig. 1B). In our analysis, the ExN and InN included several clusters (Fig. 1C), and the ExN_0 and ExN_11 also showed differences in the proportions (Fig. 1D & supplementary Fig. 1), indicating the possible effects on the subtypes of excitatory neurons. We further analyzed the featured DEGs associated with the subtypes of cells (Fig. 1E), and significant subtype signatures were observed (Fig. 1F). The Jaccard analysis on the featured DEGs showed good correlations of the clusters with previous studies[33] (Fig. 1G).

Gene expressions predicted the suppressed oxidative phosphorylation and glycogens in the DLPFC of MDD patients

The different expressional genes (DEGs) between the MDD and HC groups were identified via the Findmarkers function of the Seurat R package and the pseudobulk RNA approach via the Muscat R package (Supplementary Table 2). The volcano plot in Fig. 2A–C showed the expressions of different genes in the ExN analyzed via two approaches. And 776 were common DEGs detected via both approaches in ExN (Fig. 2D). Interestingly, most DEGs were detected on the ExN and InN (Fig. 2E), especially on the ExN_0 and ExN_11 (Fig. 2F). Part of the DEGs were related to the metabolism, indicating the possible metabolic changes in the DLPFC of MDD patients.

Next, we examined the transcriptional changes (Fig. 3A) within specific metabolic pathways, including glucose metabolism (Glucose), a sub-term of carbohydrates (Carbohydrates), respiratory electron transport term (respiratory), a sub-term of the aerobic respiration and respiratory electron transport (TCA) from the Reactome database, as well as the oxidative phosphorylation and glycolysis/gluconeogenesis from KEGG database (Supplementary Table 3). Interestingly, gene set enrichment analysis (GSEA) predicted the suppressed terms on ExNs (Fig. 3B) and InNs (Fig. 3C). Further analysis indicated that the suppression of these terms on the ASC and OPC based on the DEGs analyzed from the snRNA-seq approach (Fig. 3D) and pseudo-bulk RNA-seq analysis approach (Fig. 3E). Furthermore, we detected the suppressed terms on most of the subtypes of neurons (Fig. 3F,G). We also analyzed the connections of leading-edge genes under these terms. Interestingly, as shown in Fig. 3H, the TCA, respiratory, and oxidative phosphorylation were tightly connected, possibly related to the mitochondrial functions. At the same time, the Carbohydrates, Glucose, and glycolysis/gluconeogenesis were more related to the glycolysis, and our analysis predicted two parts of possible changes in the DLPFC of MDD patients, including the glycolysis and the respiratory. Furthermore, our results indicated that the changed leading-edge genes differed among subtypes of ExNs, and 67 genes were shared among ExN_0, ExN_2, and ExN_12 (Fig. 3I). The fold changes and the adjusted p-value of these genes are shown in Fig. 3J. We also performed the gene ontology (GO) analysis. In the biological process, we detected the enriched terms on the ATP metabolic process, oxidative phosphorylation, purine ribonucleoside triphosphate metabolic process, and aerobic respiration. The inner mitochondrial membrane protein complex, respirasome, as well as cytochrome complex, were enriched on cellular components. Furthermore, the enriched terms for the molecular functions included proton transmembrane transporter and electron transfer activity (Fig. 3K). Thus, our analysis indicated that the oxidative phosphorylation and glycolysis/gluconeogenesis may be downregulated in the DLPFC of MDD patients.

GSEA on the human phenotype ontology predicted the changed serum lactate in MDD patients

To determine whether the changed gene expressions were associated with the MDD, we subsequently explored the Human Phenotype Ontology (HPO) database, which provides a comprehensive logical standard for describing and computationally analyzing phenotypic abnormalities found in human disease[41]. We downloaded

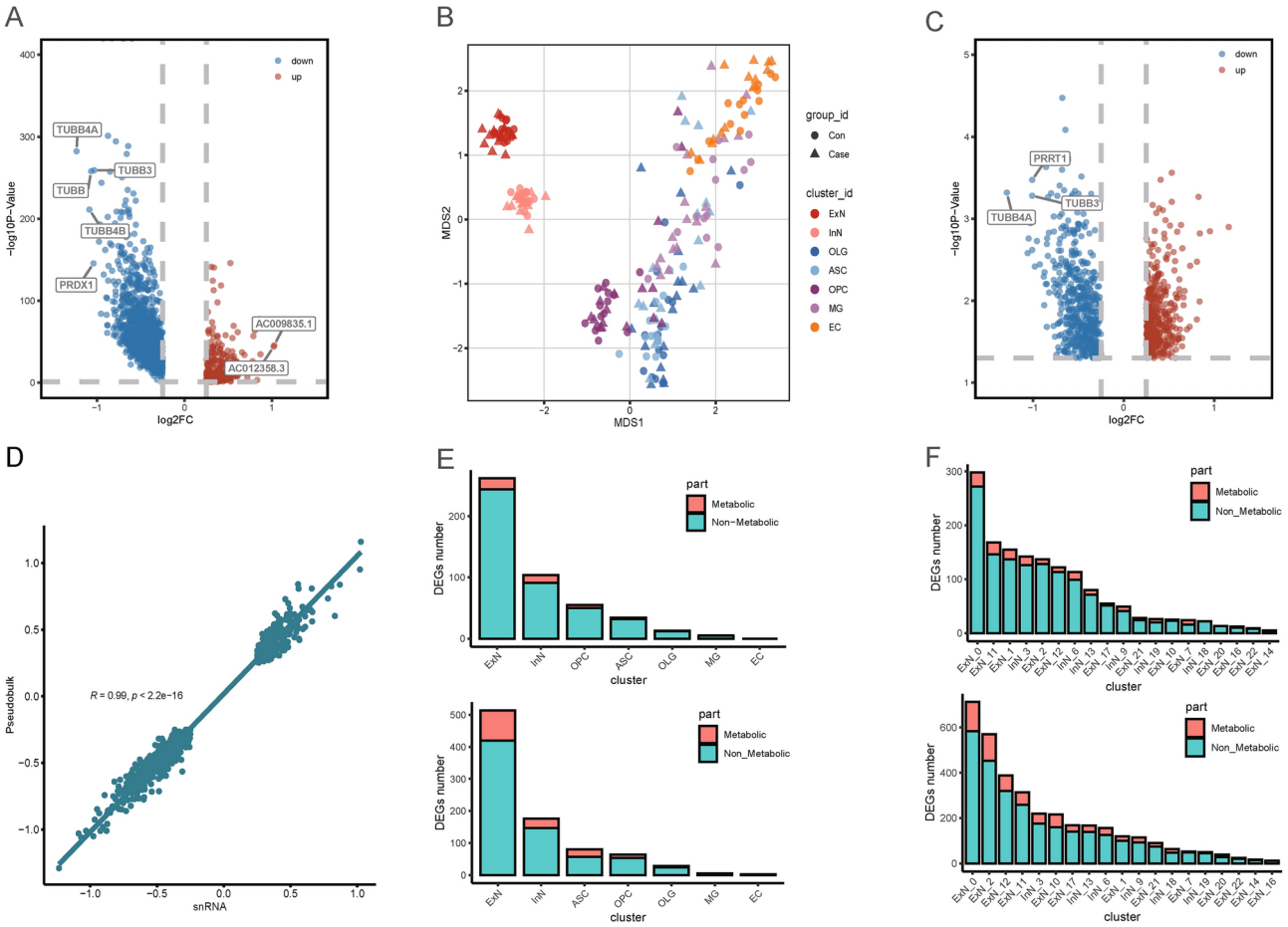

Fig. 2. Differential Expressional Changes in Genes within the DLPFC of MDD Patients. (**A**) Volcano plots depicting differentially expressed genes (DEGs) between MDD and HC groups in excitatory neurons (ExNs) analyzed using the FindMarkers function of Seurat. The x-axis represents the average log2 fold change (avg_log2FC), and the y-axis represents the negative logarithm of the adjusted p-value (-log10p_adj). (**B**) Dot plot presenting pseudobulk-level multidimensional scaling (MDS) plot. (**C**) Volcano plots illustrating differentially expressed genes (DEGs) between MDD and HC groups in excitatory neurons (ExNs) as detected by the pseudobulk approach. The x-axis represents the log2 fold change (log2FC), and the y-axis represents the negative logarithm of the adjusted p-value (-log10p_adj). (**D**) Scatterplot showing the fold changes of common DEGs derived from single nucleus RNA sequencing (snRNA-seq) and pseudobulk RNA approaches. (**E**) Bar graph displaying the number of metabolic-related DEGs across cell types, with upregulated DEGs indicated by upper heatmap and downregulated DEGs by "downset." (**F**) Bar graph illustrating the number of metabolic-related DEGs across cell subtypes, with upregulated DEGs indicated by "upset" and downregulated DEGs by lower heatmap.

the HPO terms and performed the GSEA. To narrow down the possible HPOs, we focused on terms related to depression and functions of mitochondrial and lactate changes (Supplementary Table 4). Interestingly, the suppressed HPO terms were detected in both the ExNs and InNs (Fig. 4A,B), and the GSEA results based on the DEGs detected by Seurat and pseudo-bulk RNA approach were consistent on the ExNs, but not InNs (Fig. 4C). Furthermore, we also detected the suppressed HPO terms in the subtypes of neurons, especially the ExN_0, ExN_2, and ExN_12 subtypes (Fig. 4D,E). The NES from the DEGs by Seurat were highly correlated to that from the pseudo-bulk RNA approach (Fig. 4F).

We then examined the connections between the metabolic-related genes and the HPO-related genes. As shown in Fig. 4G, the leading-edge genes of aerobic respiration and respiratory electron transport (TCA), Respiratory electron transport term (Respiratory), and oxidative phosphorylation were correlated to the HPO terms, such as the abnormal on mitochondrial respiratory chain, CSF metabolite concentration, as well as the serum and CSF lactate. We further analyzed the common genes among the TCA, respiratory, oxidative phosphorylation, and serum lactate terms (Fig. 4H). We detected 13 common genes in the ExN_0, and these related genes differed among ExN_0, ExN_2, and ExN_12 (Fig. 4I). The changed expression patterns are shown in Fig. 4J. Therefore, our results predicted the connections between the abnormal metabolism in the DLPFC and the abnormal metabolic changes in the serum and CSF.

Next, we performed flux balance analysis (FBA) and constructed genome-scale metabolic network reconstructions[39] via the METAflux R package. Glucose is the primary energy source; we then evaluated glucose's relative uptake and release rate and the reactions involved in glycolysis (Fig. 5A). As shown in Fig. 5B, glucose uptake in ExNs increased, while glucose release from ASCs and InNs decreased. Furthermore, the reaction of glucose to generate pyruvate was impaired in ASCs (Fig. 5C–L). The amount of aldolase that converts fructose 1,6-bisphosphate into glyceraldehyde 3-phosphate and dihydroxyacetone phosphate was significantly decreased in all cell types, indicating that this reaction was impaired in MDD patients. Our results also predicted a reduced reaction of the relocation of phosphate from the third to the second carbon of the phosphoglycerate in ExN; these impairments further led to the suppressed response of pyruvate generation. Pyruvate can also be converted into lactate via fermentation or as a significant substrate for the TCA cycle[42]. Interestingly, both reactions were decreased in the MDD condition (Fig. 5M,N). Interestingly, we also detected decreased lactate in both ExNs, InNs, and out medium of the MDD samples (Fig. 5O). In line with our GSEA results, the FBA results indicated the broad downregulation of glycolysis in the DLPFC of MDD patients.

Decreased serum lactate concentrations in MDD patients

Our in-silicon analysis predicted the changes in serum lactate in the MDD patients. To confirm this point, we recruited 40 MDDs and 47 HCs (Table 1) and examined the serum lactate concentrations (Supplementary Table 5). There was no difference in age between MDDs and HCs. The serum concentration of lactate in MDDs was significantly lower than that in HCs [Males: (2.39 ± 0.53) vs. (5.44 ± 0.69), $P < 0.05$; Females: (2.14 ± 0.20) vs. (4.79 ± 0.35), $P < 0.01$] (Fig. 6A). Furthermore, serum lactate concentrations were negatively correlated with age (Fig. 6B). We also examined the possible difference in Body Mass Index (BMI) and found no difference between MDDs and HCs (Fig. 6C); additionally, we did not detect a correlation between lactate and BMI (Fig. 6D). Furthermore, no correlations were detected between lactate and the HAMD (Fig. 6E) or HAMA (Fig. 6F) scores of MDD patients. Consequently, our analysis of snRNA-seq data accurately predicted the reduced serum lactate levels in MDD patients.

Discussion

In the present study, we analyzed the snRNA-seq data from MDD patients and healthy controls (HC). We revealed the downregulation of metabolism-related terms in excitatory neurons from the prefrontal cortex (DLPFC) of MDD patients. These terms include glucose metabolism (Glucose), a subset of carbohydrates metabolism (Carbohydrates), respiratory electron transport (respiratory), a sub-term of aerobic respiration and respiratory electron transport (TCA) from the Reactome database, as well as oxidative phosphorylation and glycolysis/gluconeogenesis from the KEGG database. Additionally, abnormalities in the mitochondrial respiratory chain, cerebrospinal fluid (CSF) metabolite concentrations, and serum and CSF lactate levels were identified based on the Human Phenotype Ontology (HPO) database. Confirmation of these in-silico results came from examining serum lactate concentrations, which showed a decrease in MDD patients. Our results suggest a potential impairment in energy metabolism and anabolic processes within the DLPFC of MDD patients, which could contribute to the pathophysiology of the disorder. The decrease in serum lactate further supports the hypothesis of altered energy metabolism in MDD and may have implications for diagnosing and treating the disorder.

Lactate is involved in MDD in multiple ways

Lactate, once viewed as a simple metabolic byproduct, is now recognized for its pivotal role in brain metabolism and synaptic plasticity[43]. The metabolic aspects of lactate are highlighted by its production by astrocytes and utilization by neurons, which is part of the astrocyte-neuron lactate shuttle (ANLS) hypothesis[44]. Bonvento and Bolanos (2021) discussed the compartmentalization of brain energy metabolism between astrocytes and neurons, emphasizing the role of lactate[28]. In the current study, our in-silicon analysis on the snRNA-seq data from DLPFC predicted the changes in serum lactate in MDD patients, and we further detected a decreased level of lactate in the serum of MDD patients. Our results not only showed the serum changes of lactate but also provided the transcriptomic information for the changes of lactate, which may help to understand the cellular and molecular mechanism of lactate abnormalities in MDD.

The antidepressant role of lactate has been studied extensively. Carrard et al. (2021) demonstrated that lactate reverses the depressive effects of corticosterone on behavior and adult hippocampal neurogenesis, suggesting a role in the pathophysiology of MDD[45]. El Hayek et al. (2019) showed that lactate can mediate resilience to stress and has antidepressant effects by modulating hippocampal levels and activity of histone deacetylases[46]. Shaif et al. (2018) demonstrated the antidepressant-like effect of lactate in an animal model of menopausal depression[47]. Recently, Yan et al. (2024) showed that physical exercise, known for its antidepressant effects, mediates cortical synaptic protein lactylation, improving stress resilience and preventing anxiety-like behaviors in mice under chronic stress[48]. Together, these studies suggest that lactate may be a crucial factor in the development and treatment of depression. In line with these studies, our analysis predicted the downregulation of lactate in both CSF and serum and the serum lactate was confirmed in MDD patients. Therefore, novel approaches to elevate the lactate levels in MDD patients should be developed in the future.

The role of lactate in promoting the survival and proliferation of new neurons in the hippocampus, a critical process affected in depression, is also highlighted[45]. This connection is further supported by the idea that inhibiting adult hippocampal neurogenesis prevents the antidepressant-like effects of lactate[45]. Lev-Vachnish et al. found that lactate promotes adult hippocampal neurogenesis[49]. Boldrini et al. reported that antidepressants increase neural progenitor cells in the human hippocampus, suggesting a role for neurogenesis in the action of antidepressants[50]. The current study analyzed the snRNA-seq data from the DLPFC of MDD patients, and the flux balance analysis (FBA) results in[39] via the METAflux R package indicated the decreased lactate in the ASC, ExNs and InNs in the DLPFC. Based on Karnib's study[46], the lower level of lactate may affect the activity of

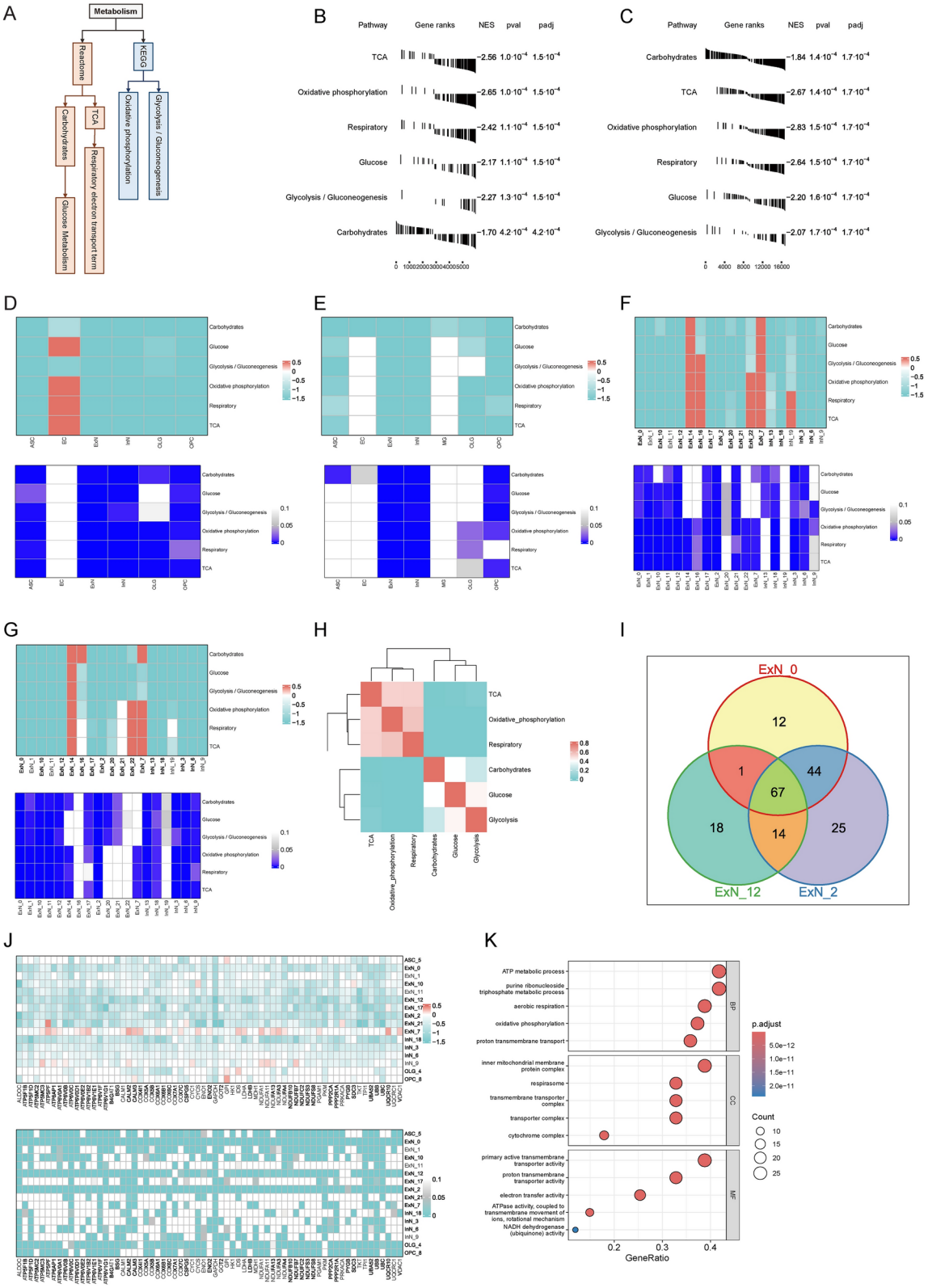

histone deacetylases and the lactification of some proteins in the PFC. And further studies need to be performed to check this point.

Lactate may serve as a signaling molecule in synaptic plasticity, memory processes, and drug addiction rather than just an energy substrate[51]. Here, our analysis based on the snRNA-seq data indicates broadly metabolic changes in the DLPFC, and the GSEA based on DEGs indicated a decreased lactate in the PFC; this suggests the communications between astrocytes and neurons may be abnormal in MDD, which further affects the synaptic plasticity. Suzuki et al. demonstrated that astrocyte-neuron lactate transport is required for long-term memory formation[52]. Yang et al. (2014) show that lactate stimulates the expression of synaptic plasticity-related genes

◀**Fig. 3**. Metabolic changes in the DLPFC of MDD patients based on KEGG and reactome database analysis. (**A**) Diagram illustrating the metabolic-related pathways selected for Gene Set Enrichment Analysis (GSEA) from the KEGG and Reactome databases. (**B**) Summary table of GSEA results for metabolic pathways in excitatory neurons (ExNs) based on differentially expressed genes (DEGs) identified using the single nucleus RNA sequencing (snRNA-seq) approach. The barcode pattern indicates the position of genes in the ranked list, with left-side bars suggesting upregulated genes at the top of the list and right-side bars indicating downregulated genes at the bottom. The enrichment score reflects the degree of gene enrichment at the top (positive) or bottom (negative) of the ranked list. (**C**) Summary table of GSEA results for metabolic pathways in excitatory neurons (ExNs) based on DEGs identified using the pseudobulk RNA approach. (**D**) Heatmaps displaying GSEA results for metabolic pathways based on DEGs identified using the snRNA-seq approach. The upper heatmap represents the normalized enrichment score (NES), and the lower heatmap represents the negative logarithm of the adjusted p-value (log10p_adj). (**E**) Heatmaps displaying GSEA results for metabolic pathways based on DEGs identified using the pseudobulk RNA approach. The upper heatmap represents the NES, and the lower heatmap represents the log10p_adj. (**F**) Heatmaps displaying GSEA results for metabolic pathways based on DEGs of cell subtypes identified using the snRNA-seq approach. The upper heatmap represents the NES, and the lower heatmap represents the log10p_adj. (**G**) Heatmaps displaying GSEA results for metabolic pathways based on DEGs of cell subtypes identified using the pseudobulk RNA approach. The upper heatmap represents the NES, and the lower heatmap represents the log10p_adj. (**H**) Heatmap indicating the overlap of genes among metabolic-related terms. (**I**) Venn diagram showing the overlap of leading-edge genes among ExN_0 (124 genes), ExN_2(150 genes), and ExN_12 (149 genes). "Leading-edge genes" are the genes that contribute most significantly to the enrichment score within a particular pathway. (**J**) Heatmaps displaying the fold changes (up) and log10p_adj (down) of common genes identified in panel I. (**K**) Dotplots showed the results of the GO enrichment analysis on the 67 common genes identified in panel I.

through NMDA receptor activity and the Erk1/2 signaling pathway[53]. Lactate modulates neurotransmission mainly through its effects on NMDA receptors, which are key to synaptic plasticity and memory formation[53]. This modulation is proposed to involve changes in the redox state of neurons, affecting their excitability. Jourdain et al. (2018) found that lactate has a dual action on the activity of NR2B-containing NMDA receptors, influencing both potentiation and neuroprotection[54]. El Hayek et al. demonstrated that lactate's effects on learning and memory are mediated through SIRT1-dependent activation of hippocampal brain-derived neurotrophic factor (BDNF)[46]. In summary, lactate is a multifunctional molecule with significant implications for understanding the neurobiology of MDD, the mechanisms of synaptic plasticity, and the development of potential therapeutic strategies targeting lactate signaling pathways.

A suppressed energy supply may affect synaptic transmission in the DLPFC of MDD patients.

Decreased synaptic transmission in the PFC of MDD patients may lead to hypoactivation of the PFC[4]. Synaptic transmission and plasticity consume most of the energy in the brain[10,55]; synaptic activity includes vesicle filling, vesicle transport, transmitter release, transmitter binding, channel opening, vesicle recycling, and enzymatic processing of synaptic transmitters within synapses, as well as maintenance of the resting membrane potential. All of these processes require energy support and consume ATP[55]. Inhibition of glycolysis, which affects the generation of presynaptic ATP, is accompanied by a reduction in neuronal transmitter release[55,56]. In the present study, our analysis predicted suppressed oxidative phosphorylation in the ACC and ExN based on the KEGG metabolic terms in the ASC and ExN of the DLPFC (Fig. 3B,C), which may affect the generation of ATP. Furthermore, our results revealed downregulated glucose and glycogen metabolism based on metabolic-related terms from the Reactome database. Moreover, FBA also confirmed the change in glycolysis, which may lead to an abnormal energy supply. Since activity-induced ATP synthesis is tightly connected to regular synaptic activity and plasticity maintenance, metabolic impairment, including oxidative phosphorylation, glucose, and glycogen metabolism, may be one factor in the hypoactivation of the DLPFC in MDD patients.

Abnormal glucose metabolism is closely associated with MDD

In the current study, the snRNA-seq data analysis predicted the suppressed glucose metabolism, carbohydrate metabolism, and glycolysis/gluconeogenesis in the DLPFC of MDD patients. Further analysis via the METAflux R package confirmed the changed glucose metabolism in different cell types. Therefore, the transcriptomic information connected the abnormal glucose metabolism to the MDD. Previous studies found that Suicide attempts in MDD patients have been related to blood glucose levels, with significantly higher levels observed in patients who had attempted suicide[57]. A prevalence of abnormal glucose metabolism of 12.57% was also found in young MDD patients, suggesting a high co-morbidity of glucose metabolism abnormalities in this population. Factors such as thyroid-stimulating hormone (TSH) levels, anxiety scores, and metabolic parameters are associated with fasting blood glucose levels in patients with first-episode medication-naïve MDD[14]. Alterations in regional cerebral metabolism affect resting-state functional connectivity in MDD, with reduced glucose metabolism in areas like the putamen, claustrum, insular, and inferior frontal gyrus[14]. The prevalence of abnormal glucose metabolism in MDD patients, its correlation with suicidality, and the impact of inflammation and insulin resistance on depressive symptoms all point toward a complex interplay between metabolic dysfunction and mental health. Taking advantage of the snRNA-seq approach, our analysis provided the cellular information related to the glucose metabolism in the DLPFC of MDD patients, which would help understand the cellular and molecular mechanism of abnormal glucose in the MDD.

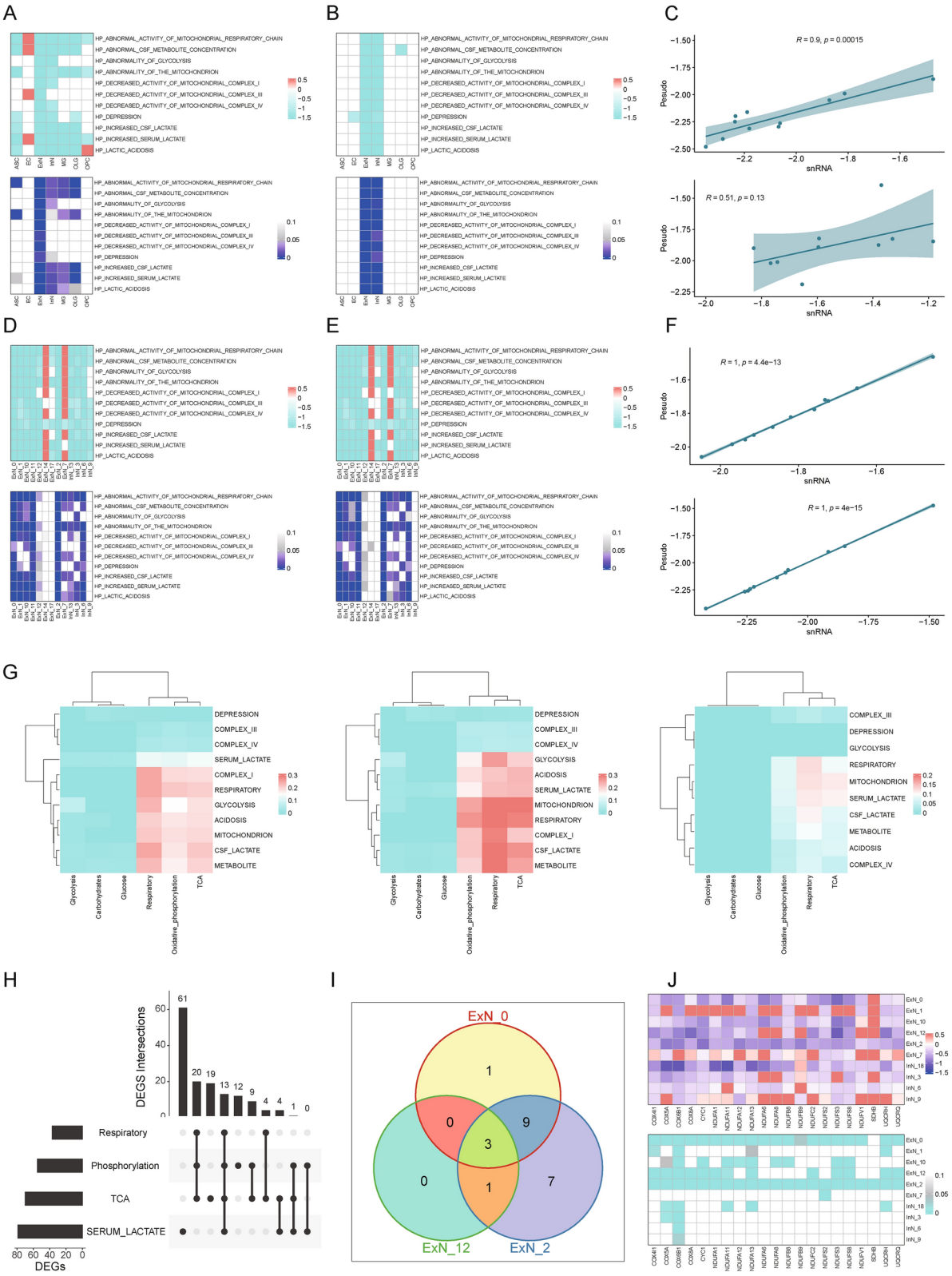

The mitochondrial dysfunction in the MDD

Mitochondrial dysfunction, characterized by alterations in the efficiency of the electron transport chain and oxidative phosphorylation, has been implicated in the pathophysiology of MDD. The tricarboxylic acid (TCA) cycle metabolites[58], part of the mitochondrial respiratory chain, have been shown to control cellular functions and fate by regulating chromatin modifications, DNA methylation, and post-translational modifications of proteins. These processes are crucial for cellular homeostasis and are increasingly recognized for their roles in physiology and disease, including MDD.

◀**Fig. 4**. Gene Set Enrichment Analysis (GSEA) Results of Human Phenotype Ontology (HPO) Based on DLPFC DEGs. (**A**) Heatmaps displaying GSEA results for HPO using differentially expressed genes (DEGs) identified via the single nucleus RNA sequencing (snRNA-seq) approach. The upper heatmap represents the normalized enrichment score (NES), and the lower heatmap represents the negative logarithm of the adjusted p-value (log10p_adj). (**B**) Heatmaps displaying GSEA results for HPO using DEGs identified via the pseudobulk RNA approach. The upper heatmap represents the NES, and the lower heatmap represents the log10p_adj. (**C**) Scatterplot illustrating the correlations between the NES of GSEA results based on DEGs from the Seurat approach and pseudobulk RNA approaches for excitatory neurons (ExNs) (upper) and inhibitory neurons (InNs) (lower). (**D**) Heatmaps displaying GSEA results for HPO using DEGs from cell subtypes identified via the snRNA-seq approach. The upper heatmap represents the NES, and the lower heatmap represents the log10p_adj. (**E**) Heatmaps displaying GSEA results for HPO using DEGs from cell subtypes identified via the pseudobulk RNA approach. The upper heatmap represents the NES, and the lower heatmap represents the log10p_adj. (**F**) Scatterplot illustrating the correlations between the NES of GSEA results based on DEGs from the Seurat approach and pseudobulk RNA approaches for ExN subtypes ExN_0 (upper) and ExN_2 (lower). (**G**) Heatmaps demonstrating the overlap of leading-edge genes between metabolic-related terms and HPO-related terms. Left for ExN_0, middle for ExN_2, and right panel for ExN_12. (**H**) Upset plot showing the overlap of leading-edge genes for the serum lactate and metabolic-related terms specific to ExN_0. (**I**) Venn diagram displaying the overlap of leading-edge genes among ExN_0, ExN_2, and ExN_12 subtypes. (**J**) Heatmaps displaying the fold changes (up) and log10p_adj (down) of genes identified in panel I.

Here, our GSEA on the metabolic terms from the KEGG and Reactome databases indicated the Mitochondrial dysfunction in the DLPFC of MDD patients, including the suppressed electron transport chain functions and oxidative phosphorylation. The GSEA based on HPO also suggests Mitochondrial dysfunction, especially in the Mitochondrial complex I, III and VI, indicating the close connections between Mitochondrial functions and MDD. Furthermore, studies have reported altered bioenergetics in MDD patients, including decreased respiration and mitochondrial membrane potential (MMP), consistent with mitochondrial dysfunction[59]. Studies have shown associations between MDD and changes in mitochondrial biogenesis, redox imbalance, increased oxidative damage to cellular macromolecules, and apoptosis[60]. Specifically, alterations in the activity of respiratory chain enzymes, such as complexes I-IV, and changes in the mitochondrial DNA copy number have been observed in patients with MDD compared to HCs[61,62]. These findings suggest that mitochondrial respiratory chain function may influence treatment response in MDD. Further research is needed to understand the molecular networks and biological mechanisms involving mitochondria in MDD and to explore the potential of mitochondrial function as a biomarker or therapeutic target in the disorder[60,62,63].

Limitations of the study

The study conducted to explore potential metabolic alterations in the DLPFC of MDD patients using snRNA-seq data analysis has several limitations that warrant acknowledgment. Firstly, while the analysis identified suppressed metabolic terms such as glucose and carbohydrate metabolism, oxidative phosphorylation, and glycolysis/gluconeogenesis based on gene expression data, the study was limited by the inability to obtain patient brain samples for direct confirmation of differential gene expression. This constraint prevented the validation of in-silico findings through direct biological assays or histopathological examinations, which could have strengthened the conclusions drawn from the gene expression data.

Additionally, the study relied on predictions from the Human Phenotype Ontology (HPO) database to infer changes in lactate levels in serum and cerebrospinal fluid (CSF), which, while informative, are not a direct measure of metabolic activity within the brain. The reliance on serum lactate as a proxy for brain metabolic changes is a significant limitation, as peripheral markers may not accurately reflect central nervous system metabolism. Since we focused on the possible metabolic changes in the DLPFC of MDD patients, we performed the GSEA pathway analysis, which focused only on specific metabolic pathways. Although these metabolic terms were also detected when using the whole KEGG terms, they may lead to potential biases.

Moreover, while the study provided transcriptional evidence for metabolic changes in the DLPFC of MDD patients, it did not directly address the causal role of these metabolic changes in the development or progression of MDD. The correlation between metabolic alterations and the pathophysiology of MDD requires further investigation through longitudinal studies and mechanistic experiments to establish a clear causal link. Furthermore, here, we detected the slightly negative correlations between lactate and age, which the decreased practice or hormone changes may cause, and these connections should also be studied in the future.

In summary, while the study offers valuable insights into potential metabolic dysregulation in MDD, it is imperative to conduct additional experiments, including in vivo studies and possibly clinical trials, to substantiate these findings and to elucidate the precise role of metabolic changes in the etiology and treatment of MDD. Addressing these limitations will be crucial for advancing our understanding of the disorder and developing targeted therapeutic strategies.

Conclusion

In conclusion, the present study has shed light on the intricate relationship between MDD and metabolic dysregulation, particularly highlighting the downregulation of metabolism-related terms in excitatory neurons from the DLPFC of MDD patients; this includes key processes such as glucose metabolism, carbohydrate metabolism, respiratory electron transport, and the tricarboxylic acid (TCA) cycle, which are essential for energy production and cellular respiration[64]. The study's findings of abnormalities in the mitochondrial respiratory

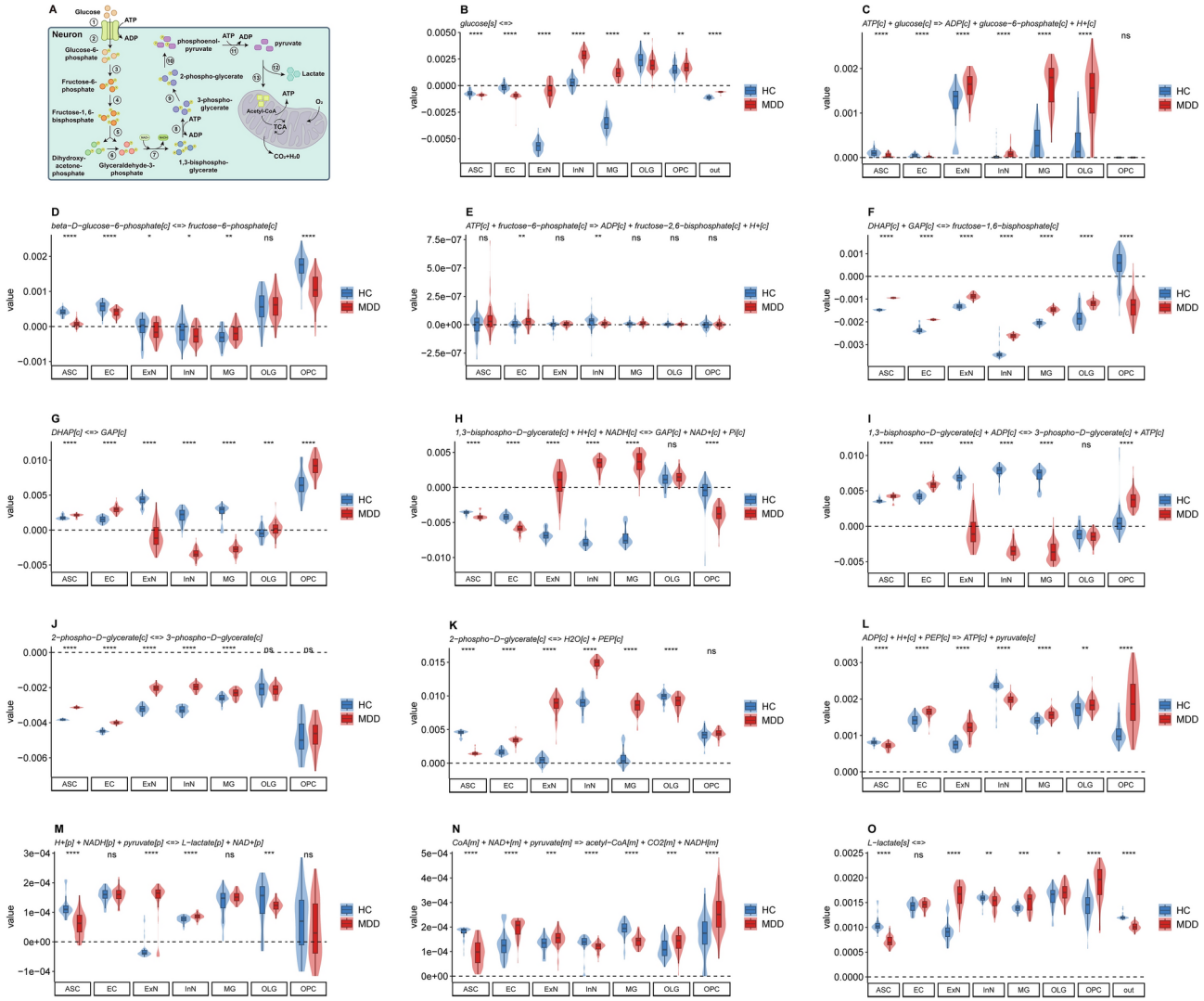

Fig. 5. Possible changes in glycolysis-related metabolites. (**A**) Diagram showing glucose uptake and the major glycolysis reactions. (**B**) Violin plot showing the difference in glucose uptake and release between the HC and MDD groups. A positive value indicates a release of glucose, and a negative value suggests glucose uptake. (**C**–**L**) Violin plots representing the possible differences in glycolysis reactions, including reactions 2 to 11. A positive value implies that the net flux is in the forward direction, and a negative value indicates that the net flux is in the backward direction. Absolute values denote the magnitude of the flux. (**M**) The predicted generation of lactate from pyruvate in different cell types. (**N**) Violin plot showing the possible suppression of acetyl-CoA generation in the DLPFC of MDD patients. (**O**) The release of lactate may be decreased in the ExN and InNs in the DLPFC of MDD patients. Note: The central line of box plots represents the median, and the boxes represent the Interquartile range (IQR).

	MDDs (n = 40)		HCs (n = 47)		*P* values	
	Males (n = 9)	Females (n = 31)	Males (n = 11)	Females (n = 36)	1.000#a	
Age (years)	24.22 ± 3.22	27.83 ± 1.93	24.45 ± 2.53	28.25 ± 1.93	0.956#b	0.887#c
HAMD	27.11 ± 1.24	28.16 ± 1.01	–	–		
HAMA	20.78 ± 1.00	20.74 ± 0.84	–	–		
Lactate (pg/mL)	2.30 (1.94–2.58)	1.95 (1.47–2.58)	4.95 (3.81–5.79)	3.98 (3.28–5.79)	< 0.001#b&#d	< 0.001#c&#d

Table 1. Differences in lactate concentrations in MDD and HC groups. Note: #a: No difference on the gender distribution compared by Pearson's Chi-squared test; #b: Compared between males. #c: Compared between females; #d: A Wilcoxon test was used, the concentrations of lactate were reported as median (Q1–Q3).

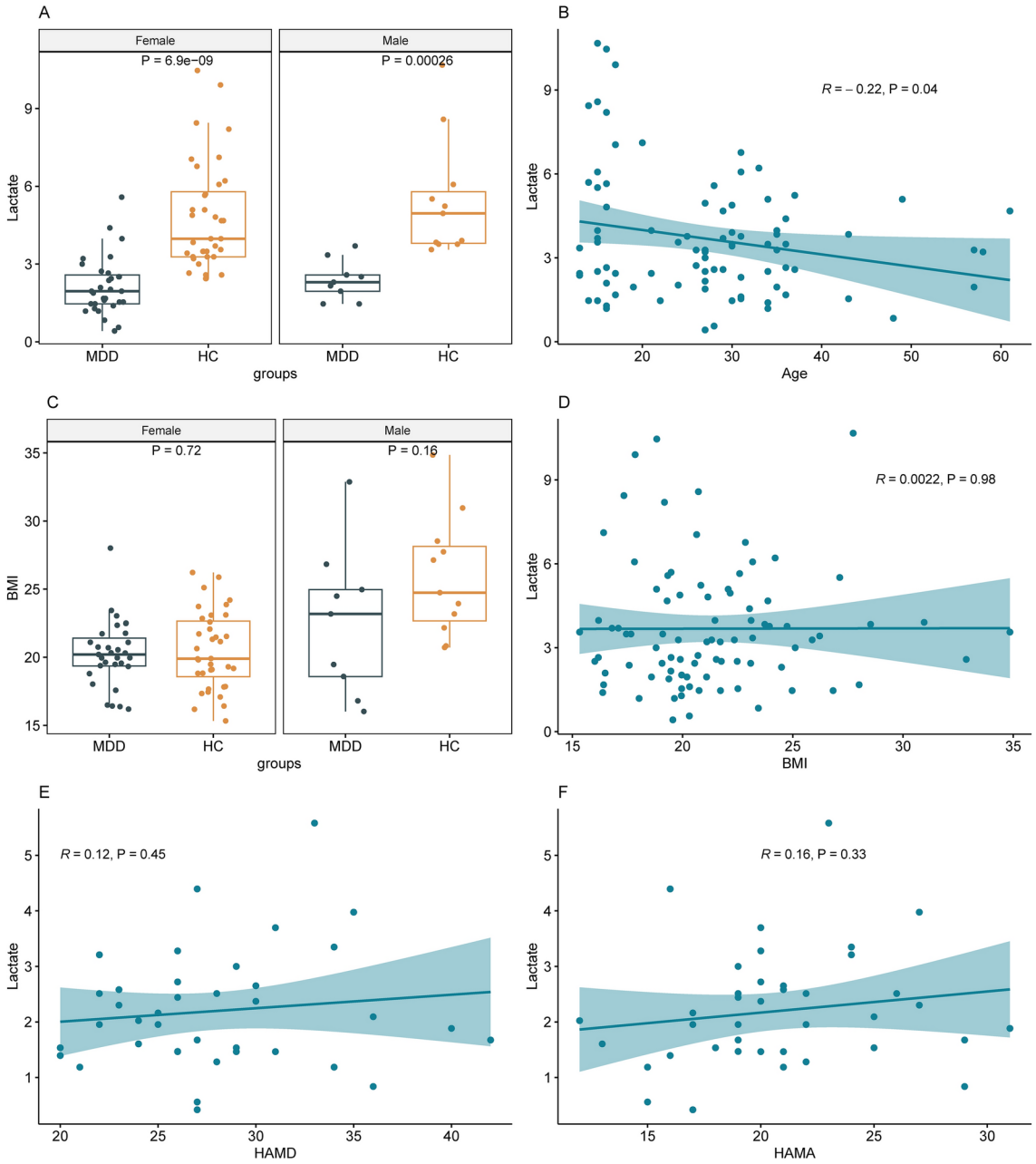

Fig. 6. Serum Lactate Levels and Correlations in Major Depressive Disorder (MDD) Patients. (**A**) Boxplots displaying lower levels of serum lactate in MDD compared to HCs. (**B**) Scatterplot illustrating the negative correlation between serum lactate concentrations and patient age. (**C**) Boxplots displaying no difference in the BMI in MDD compared to HCs. (**D**) No significant correlation between serum lactate concentrations and BMI in MDD group. (**E**) Scatterplot showing no significant correlation between serum lactate concentrations and Hamilton Depression Rating Scale (HAMD) scores in the MDD group. (**F**) Scatterplot showing no significant correlation between serum lactate concentrations and Hamilton Anxiety Scale (HAMA) scores in the MDD group.

chain, cerebrospinal fluid (CSF) metabolite concentrations, and serum and CSF lactate levels underscore the potential impairment in energy metabolism within the DLPFC of MDD patients. The decreased serum lactate concentrations observed in MDD patients further support the hypothesis of altered energy metabolism, which may have significant implications for diagnosing and treating MDD. These results contribute to the growing body of evidence suggesting that metabolic disturbances are not only prevalent in MDD but also play a crucial role in its pathophysiology, potentially offering new avenues for therapeutic intervention and a deeper understanding of the disorder's complexity.

Data availability

The raw data for this bioinformatics analysis all come from the GEO database, with specific accession numbers of GSE144136. The code and data generated in this study are available from the corresponding author on reasonable request.

Received: 16 November 2024; Accepted: 25 February 2025
Published online: 03 March 2025

References

1. Bains, N. & Abdijadid, S. Major depressive disorder. In Treasure Island (FL) (2023).
2. McLachlan, G. Treatment resistant depression: what are the options?. *BMJ* **363**, k5354 (2018).
3. Voineskos, D., Daskalakis, Z. J. & Blumberger, D. M. Management of Treatment-Resistant Depression: Challenges and Strategies. *Neuropsychiatr. Dis. Treat.* **16**, 221–234 (2020).
4. Pizzagalli, D. A. & Roberts, A. C. Prefrontal cortex and depression. *Neuropsychopharmacology* **47**, 225–246 (2022).
5. Parekh, P. K., Johnson, S. B. & Liston, C. Synaptic mechanisms regulating mood state transitions in depression. *Annu. Rev. Neurosci.* **45**, 581–601 (2022).
6. Kim, S. Y. et al. Childhood abuse and cortical gray matter volume in patients with major depressive disorder. *Psychiatry Res.* **319**, 114990 (2023).
7. Csabai, D., Wiborg, O. & Czéh, B. Reduced synapse and axon numbers in the prefrontal cortex of rats subjected to a chronic stress model for depression. *Front. Cell. Neurosci.* **12**, 24 (2018).
8. Moda-Sava, R. N. et al. Sustained rescue of prefrontal circuit dysfunction by antidepressant-induced spine formation. *Science* **364**, eaat8078 (2019).
9. Thompson, S. M. et al. An excitatory synapse hypothesis of depression. *Trends Neurosci.* **38**, 279–294 (2015).
10. Harris, J. J., Jolivet, R. & Attwell, D. Synaptic energy use and supply. *Neuron* **75**, 762–777 (2012).
11. Li, S., Xiong, G. J., Huang, N. & Sheng, Z. H. The cross-talk of energy sensing and mitochondrial anchoring sustains synaptic efficacy by maintaining presynaptic metabolism. *Nat. Metab.* **2**, 1077–1095 (2020).
12. Chen, H., Xie, L., Wang, Y. & Zhang, H. Postsynaptic potential energy as determinant of synaptic plasticity. *Front. Comput. Neurosci.* **16**, 1–11 (2022).
13. Mocking, R. J. T. et al. Biological profiling of prospective antidepressant response in major depressive disorder: Associations with (neuro)inflammation, fatty acid metabolism, and amygdala-reactivity. *Psychoneuroendocrinology* **79**, 84–92 (2017).
14. Chen, Y. H., Wang, H. N., Lang, X. E. & Zhang, X. Y. Prevalence and clinical correlates of abnormal glucose metabolism in young, first- episode and medication-naïve outpatients with major depressive disorder. *Psychiatry Res.* **325**, 115250 (2023).
15. Lu, X. et al. Biochemical metabolism in the anterior cingulate cortex and cognitive function in major depressive disorder with or without insomnia syndrome. *J. Affect. Disord.* **335**, 256–263 (2023).
16. Chirico, M. et al. Kynurenine pathway metabolites selectively associate with impaired associative memory function in depression. *Brain Behav. Immun. Heal.* **8**, 100126 (2020).
17. Meier, T. B. et al. Relationship between neurotoxic kynurenine metabolites and reductions in right medial prefrontal cortical thickness in major depressive disorder. *Brain Behav. Immun.* **53**, 39–48 (2016).
18. Young, K. D. et al. Kynurenine pathway metabolites are associated with hippocampal activity during autobiographical memory recall in patients with depression. *Brain Behav. Immun.* **56**, 335–342 (2016).
19. Lewis, C. P. et al. Altered anterior cingulate glutamatergic metabolism in depressed adolescents with current suicidal ideation. *Transl. Psychiatry* **10**, 119 (2020).
20. Jones, J. S. et al. Evaluation of brain structure and metabolism in currently depressed adults with a history of childhood trauma. *Transl. Psychiatry* **12**, 392 (2022).
21. Pan, L. A. et al. Metabolic features of treatment-refractory major depressive disorder with suicidal ideation. *Transl. Psychiatry* **13**, 393 (2023).
22. Zhang, S. et al. Cognitive dysfunction in diabetes: abnormal glucose metabolic regulation in the brain. *Front. Endocrinol. (Lausanne)* **14**, 1–14 (2023).
23. Murphy-Royal, C. et al. Stress gates an astrocytic energy reservoir to impair synaptic plasticity. *Nat. Commun.* **11**, 2014 (2020).
24. Stapel, B. et al. Impact of fasting on stress systems and depressive symptoms in patients with major depressive disorder: a cross-sectional study. *Sci. Rep.* **12**, 1–10 (2022).
25. Wu, A., Lee, D. & Xiong, W. C. Lactate metabolism, signaling, and function in brain development, synaptic plasticity, angiogenesis, and neurodegenerative diseases. *Int. J. Mol. Sci.* **24**, 13398 (2023).
26. Chamaa, F., Magistretti, P. J. & Fiumelli, H. Astrocyte-derived lactate in stress disorders. *Neurobiol. Dis.* **192**, 106417 (2024).
27. Yang, C., Pan, R.-Y., Guan, F. & Yuan, Z. Lactate metabolism in neurodegenerative diseases. *Neural Regen. Res.* **19**, 69–74 (2024).
28. Bonvento, G. & Bolaños, J. P. Astrocyte-neuron metabolic cooperation shapes brain activity. *Cell Metab.* **33**, 1546–1564 (2021).
29. Chehimi, S. N., Crist, R. C. & Reiner, B. C. unraveling psychiatric disorders through neural single-cell transcriptomics approaches. *Genes (Basel)* **14**, 771 (2023).
30. Hashikawa, Y. et al. Transcriptional and Spatial Resolution of Cell Types in the Mammalian Habenula. *Neuron* **106**, 743-758.e5 (2020).
31. Anderson, K. M. et al. Convergent molecular, cellular, and cortical neuroimaging signatures of major depressive disorder. *Proc. Natl. Acad. Sci. U. S. A.* **117**, 25138–25149 (2020).
32. Nagy, C. et al. Single-nucleus transcriptomics of the prefrontal cortex in major depressive disorder implicates oligodendrocyte precursor cells and excitatory neurons. *Nat. Neurosci.* **23**, 771–781 (2020).
33. Maitra, M. et al. Cell type specific transcriptomic differences in depression show similar patterns between males and females but implicate distinct cell types and genes. *Nat. Commun.* **14**, 2912 (2023).
34. Zheng, P. et al. Integrated spatial transcriptome and metabolism study reveals metabolic heterogeneity in human injured brain. *Cell Rep. Med.* **4**, 101057 (2023).
35. Lian, Y., Wu, C., Liu, L. & Li, X. Prediction of cell-cell communication patterns of dorsal root ganglion cells : Single-cell RNA sequencing data analysis. *Neural Regen. Res.* **19**, 1–8 (2024).
36. McGinnis, C. S., Murrow, L. M. & Gartner, Z. J. DoubletFinder: Doublet detection in single-cell RNA sequencing data using artificial nearest neighbors. *Cell Syst.* **8**, 329-337.e4 (2019).
37. Croft, D. et al. Reactome: a database of reactions, pathways and biological processes. *Nucleic Acids Res.* **39**, D691–D697 (2011).
38. Breiman, L. Random forests. *Mach. Learn.* **45**, 5–32 (2001).
39. Orth, J. D., Thiele, I. & Palsson, B. Ø. What is flux balance analysis?. *Nat. Biotechnol.* **28**, 245–248 (2010).
40. Robinson, J. L. et al. An atlas of human metabolism. *Sci. Signal.* **13**, eaaz1482 (2020).
41. Köhler, S. et al. The human phenotype ontology in 2021. *Nucleic Acids Res.* **49**, D1207–D1217 (2021).
42. Baker, S. A. & Rutter, J. Metabolites as signalling molecules. *Nat. Rev. Mol. Cell Biol.* **24**, 355–374 (2023).
43. Cauli, B., Dusart, I. & Li, D. Lactate as a determinant of neuronal excitability, neuroenergetics and beyond. *Neurobiol. Dis.* **184**, 106207 (2023).

44. Pellerin, L. & Magistretti, P. J. Glutamate uptake into astrocytes stimulates aerobic glycolysis: A mechanism coupling neuronal activity to glucose utilization. *Proc. Natl. Acad. Sci. U. S. A.* **91**, 10625–10629 (1994).
45. Carrard, A. et al. Role of adult hippocampal neurogenesis in the antidepressant actions of lactate. *Mol. Psychiatry* **26**, 6723–6735 (2021).
46. Karnib, N. et al. Lactate is an antidepressant that mediates resilience to stress by modulating the hippocampal levels and activity of histone deacetylases. *Neuropsychopharmacology* **44**, 1152–1162 (2019).
47. Shaif, N. A. et al. The antidepressant-like effect of lactate in an animal model of menopausal depression. *Biomedicines* **6**, 108 (2018).
48. Yan, L. et al. Physical exercise mediates cortical synaptic protein lactylation to improve stress resilience. *Cell Metab.* **36**, 2104-2117. e4 (2024).
49. Lev-Vachnish, Y. et al. L-lactate promotes adult hippocampal neurogenesis. *Front. Neurosci.* **13**, 1–13 (2019).
50. Boldrini, M. et al. Antidepressants increase neural progenitor cells in the human hippocampus. *Neuropsychopharmacology* **34**, 2376–2389 (2009).
51. Wang, Q., Hu, Y., Wan, J., Dong, B. & Sun, J. Lactate: A novel signaling molecule in synaptic plasticity and drug addiction. *BioEssays* **41**, 1900008 (2019).
52. Suzuki, A. et al. Astrocyte-neuron lactate transport is required for long-term memory formation. *Cell* **144**, 810–823 (2011).
53. Yang, J. et al. Lactate promotes plasticity gene expression by potentiating NMDA signaling in neurons. *Proc. Natl. Acad. Sci. U. S. A.* **111**, 12228–12233 (2014).
54. Jourdain, P. et al. Dual action of L-Lactate on the activity of NR2B-containing NMDA receptors: from potentiation to neuroprotection. *Sci. Rep.* **8**, 1–16 (2018).
55. Bordone, M. P. et al. The energetic brain—A review from students to students. *J. Neurochem.* **151**, 139–165 (2019).
56. Rangaraju, V., Calloway, N. & Ryan, T. A. Activity-driven local ATP synthesis is required for synaptic function. *Cell* **156**, 825–835 (2014).
57. Zhu, Q. et al. Prevalence and clinical correlates of abnormal lipid metabolism in first-episode and drug-naïve patients with major depressive disorder with abnormal glucose metabolism. *Sci. Rep.* **13**, 1–8 (2023).
58. Martínez-Reyes, I. & Chandel, N. S. Mitochondrial TCA cycle metabolites control physiology and disease. *Nat. Commun.* **11**, 1–11 (2020).
59. Cardon, I. et al. Mitochondrial and cellular function in fibroblasts, induced neurons, and astrocytes derived from case study patients: Insights into major depression as a mitochondria-associated disease. *Int. J. Mol. Sci.* **25**, 963 (2024).
60. Rappeneau, V., Wilmes, L. & Touma, C. Molecular correlates of mitochondrial dysfunctions in major depression: Evidence from clinical and rodent studies. *Mol. Cell. Neurosci.* **109**, 103555 (2020).
61. Fernström, J. et al. Blood-based mitochondrial respiratory chain function in major depression. *Transl. Psychiatry* **11**, 1–7 (2021).
62. Gamradt, S. et al. Reduced mitochondrial respiration in T cells of patients with major depressive disorder. *iScience* **24**, 103312 (2021).
63. Fernström, J. et al. Mitochondrial Respiratory Chain Function in Major Depression. *Biol. Psychiatry* **87**, S197–S198 (2020).
64. Weckmann, K. et al. Ketamine's antidepressant effect is mediated by energy metabolism and antioxidant defense system. *Sci. Rep.* **7**, 1–11 (2017).

Acknowledgements

This work was supported by the National Natural Science Foundation Project of China (32271042), Key R&D Program of Zhejiang (2024SSYS0016), the National Key Research and Development Program of China (2023YFC2506200), the Fundamental Research Funds for the Central Universities (2023ZFJH01-01, 2024ZFJH01-01).

Author contributions

Y.LU and XY.LI designed experiments, analyzed data, approved the draft, and wrote the paper. G.H Li, L. He, Y. Wang, and C. Pei analyzed the snRNA-seq data, approved the draft, and wrote the paper, Y. Rao, W. He, P. Fang, L Xi and H Xie collected the patients samples and performed the Elisa experiments.

Declarations

Competing interests

The authors declare no competing interests.

Additional information

Supplementary Information The online version contains supplementary material available at https://doi.org/10.1038/s41598-025-92030-8.

Correspondence and requests for materials should be addressed to X.-Y.L. or Y.-R.L.